Article

On the Development of Sensor Molecules that Display Fe-amplified Fluorescence

Julia L. Bricks, Anton Kovalchuk, Christian Trieflinger, Marianne Nofz, Michael Bschel, Alexei I. Tolmachev, Jrg Daub, and Knut Rurack

J. Am. Chem. Soc., **2005**, 127 (39), 13522-13529• DOI: 10.1021/ja050652t • Publication Date (Web): 13 September 2005

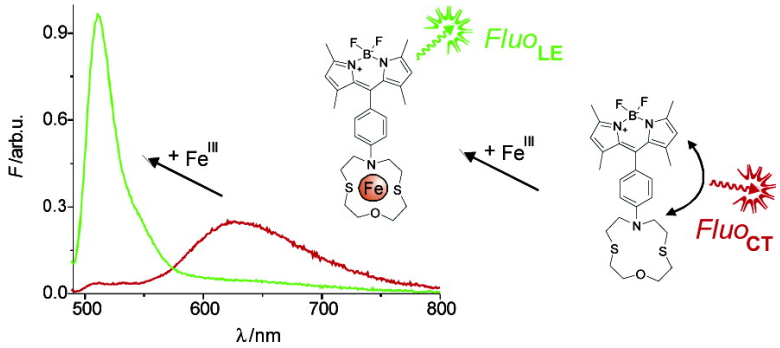

More About This Article

Additional resources and features associated with this article are available within the HTML version:

- Supporting Information
- Links to the 21 articles that cite this article, as of the time of this article download
- Access to high resolution figures
- Links to articles and content related to this article
- Copyright permission to reproduce figures and/or text from this article

View the Full Text HTML

J|A|C|S
ARTICLES
Published on Web 09/13/2005

On the Development of Sensor Molecules that Display Fe^{III}-amplified Fluorescence

Julia L. Bricks,*,† Anton Kovalchuk,‡ Christian Trieflinger,§ Marianne Nofz,‡ Michael Büschel,§ Alexei I. Tolmachev,† Jörg Daub,*,§ and Knut Rurack*,‡

Contribution from the Institute of Organic Chemistry, National Academy of Sciences of the Ukraine, 5 Murmanskaya Street, 02094 Kiev, Ukraine, Div. I.3 and V.4, Federal Institute for Materials Research and Testing (BAM), Richard-Willstätter-Strasse 11, D-12489 Berlin, Germany, Institute of Organic Chemistry, University of Regensburg, D-93040 Regensburg, Germany

Received February 1, 2005; E-mail: knut.rurack@bam.de; joerg.daub@chemie.uni-regensburg.de; timophei@bricks.kiev.ua

Abstract: Incorporation of a tailor-made size-restricted dithia-aza-oxa macrocycle, 1-oxa-4,10-dithia-7-aza-cyclododecane, via a phenyl linker into two fluorescent sensor molecules with electronically decoupled, rigidly fixed, and sterically preoriented architectures, a 1,3,5-triaryl-Δ^2-pyrazoline and a *meso*-substituted boron-dipyrromethene (BDP), yields amplified fluorescence in the red-visible spectral range upon binding of Fe^{III} ions. The response to Fe^{III} and potentially interfering metal ions is studied in highly polar aprotic and protic solvents for both probes as well as in neat and buffered aqueous solution for one of the sensor molecules, the BDP derivative. In organic solvents, the fluorescence of both indicators is quenched by an intramolecular charge or electron transfer in the excited state and coordination of Fe^{III} leads to a revival of their fluorescence without pronounced spectral shifts. Most remarkably, the unbound BDP derivative shows dual emission in water and can be employed for the selective ratiometric signaling of Fe^{III} in buffered aqueous solutions.

Introduction

In recent years, the search for selective and sensitive fluorescent probes for metal ions has tremendously gained in importance.[1] Besides the development of fluoroionophores for physiologically relevant main group I and II metal ions,[2] significant progress has been made in the design of fluorescent molecular sensors and switches for heavy and transition metal ions.[3] In particular, thiophilic ions[4] such as Hg^{II} and Ag^{I} as well as "soft"[5] transition metal ions that head the Irving−Williams order[6] of complex stabilities, e.g., Cu^{II} and Zn^{II},[7] have received constantly growing attention. Examples of specific molecular fluorosensors for less aminophilic metal ions that are at the bottom of this order, e.g., Fe^{III}, are still scarce.[8−12] This is surprising as especially Fe^{III} for instance plays a key role in many biochemical processes at the cellular level.[13] Iron is indispensable for most organisms, and both its deficiency and overload can induce various disorders[14] with iron trafficking,

† National Academy of Sciences of the Ukraine.
‡ Federal Institute for Materials Research and Testing (BAM).
§ University of Regensburg.

(1) de Silva, A. P.; Gunaratne, H. Q. N.; Gunnlaugsson, T.; Huxley, A. J. M.; McCoy, C. P.; Rademacher, J. T.; Rice, T. E. *Chem. Rev.* **1997**, *97*, 1515−1566. Valeur, B.; Leray, I. *Coord. Chem. Rev.* **2000**, *205*, 3−40. de Silva, A. P.; McCaughan, B.; McKinney, B. O. F.; Querol, M. *Dalton Trans.* **2003**, 1902−1913.
(2) Tsien, R. Y. *Methods Cell Biol.* **1989**, *30*, 127−156. Brownlee, C. *Trends Cell Biol.* **2000**, *10*, 451−457.
(3) Fabbrizzi, L.; Licchelli, M.; Pallavicini, P.; Sacchi, D.; Taglietti, A. *Analyst* **1996**, *121*, 1763−1768. Bargossi, C.; Fiorini, M. C.; Montalti, M.; Prodi, L.; Zaccheroni, N. *Coord. Chem. Rev.* **2000**, *208*, 17−32. Rurack, K. *Spectrochim. Acta, Part A* **2001**, *57*, 2161−2195.
(4) For recent representative examples, see: Nolan, E. M.; Lippard, S. J. *J. Am. Chem. Soc.* **2003**, *125*, 14270−14271. Liu, W.; Jiao, T.; Li, Y.; Liu, Q.; Tan, M.; Wang, H.; Wang, L. *J. Am. Chem. Soc.* **2004**, *126*, 2280−2281. Moon, S. Y.; Youn, N. J.; Park, S. M.; Chang, S. K. *J. Org. Chem.* **2005**, *70*, 2394−2397.
(5) According to the HSAB concept of "hard and soft acids and bases", Pearson, R. G. *J. Am. Chem. Soc.* **1963**, *85*, 3533−3539.
(6) Irving, H.; Williams, R. J. P. *Nature* **1948**, *162*, 746−747.
(7) Krämer, R. *Angew. Chem., Int. Ed.* **1998**, *37*, 772−773. Kimura, E.; Koike, T. *Chem. Soc. Rev.* **1998**, *27*, 179−184. Jiang, P. J.; Guo, Z. J. *Coord. Chem. Rev.* **2004**, *248*, 205−229.
(8) For reviews on fluorescent iron indicators, see: Espósito, B. P.; Epsztejn, S.; Breuer, W.; Cabantchik, Z. I. *Anal. Biochem.* **2002**, *304*, 1−18. Reynolds, I. J. *Ann. N. Y. Acad. Sci.* **2004**, *1012*, 27−36.
(9) For iron-responsive fluorescent probes, see: Weizman, H.; Ardon, O.; Mester, B.; Libman, J.; Dwir, O.; Hadar, Y.; Chen, Y.; Shanzer, A. *J. Am. Chem. Soc.* **1996**, *118*, 12386−12375. Nudelman, R.; Ardon, O.; Hadar, Y.; Chen, Y.; Libman, J.; Shanzer, A. *J. Med. Chem.* **1998**, *41*, 1671−1678. Hankovszky, O. H.; Kalai, T.; Hideg, E.; Jeko, J.; Hideg, K. *Synth. Commun.* **2001**, *31*, 975−986. Petrat, F.; Weisheit, D.; Lensen, M.; de Groot, H.; Sustmann, R.; Rauen, U. *Biochem. J.* **2002**, *362*, 137−147. Ma, Y.; Luo, W.; Quinn, P. J.; Liu, Z.; Hider, R. C. *J. Med. Chem.* **2004**, *47*, 6349−6362. Tumambac, G. E.; Rosencrance, C. M.; Wolf, C. *Tetrahedron* **2004**, *60*, 11293−11297. Ouchetto, H.; Dias, M.; Mornet, R.; Lesuisse, E.; Camadro, J. M. *Bioorg. Med. Chem.* **2005**, *13*, 1799−1803.
(10) For iron-responsive fluorescent sensory polymers, see: Lee, T. S.; Yang, C.; Park, W. H. *Macromol. Rapid Commun.* **2000**, *21*, 951−955. Grabchev, I.; Chovelon, J. M.; Bojinov, V. *Polym. Adv. Technol.* **2004**, *15*, 382−386. Sumner, J. P.; Kopelman, R. *Analyst* **2005**, *130*, 528−533.
(11) A number of unspecific fluorescent sensor molecules or sensory polymers that also respond to ionic iron have been reported lately as well, see: Ramachandram, B.; Samanta, A. *Chem. Commun.* **1997**, 1037−1038. Ghosh, P.; Bharadwaj, P. K.; Roy, J.; Ghosh, S. *J. Am. Chem. Soc.* **1997**, *119*, 11903−11909. Alvaro, M.; García, H.; Palomares, E.; Achour, R.; Moussaif, A.; Zniber, R. *Chem. Phys. Lett.* **2001**, *350*, 240−246. Sankaran, N. B.; Banthia, S.; Das, A.; Samanta, A. *New J. Chem.* **2002**, *26*, 1529−1531. Qian, X.; Xiao, Y. *Tetrahedron Lett.* **2002**, *43*, 2991−2994. Tarazi, L.; Narayanan, N.; Sowell, J.; Patonay, G.; Strekowski, L. *Spectrochim. Acta, Part A* **2002**, *58*, 257−264. Liu, J.-M.; Zheng, Q.-Y.; Yang, J.-L.; Chen, C.-F.; Huang, Z.-T. *Tetrahedron Lett.* **2002**, *43*, 9209−9212. Grabchev, I.; Chovelon, J.-M.; Qian, X. *New J. Chem.* **2003**, *27*, 337−340. Grabchev, I.; Chovelon, J. M.; Qian, X. *J. Photochem. Photobiol. A* **2003**, *158*, 37−43.

 10.1021/ja050652t CCC: $30.25

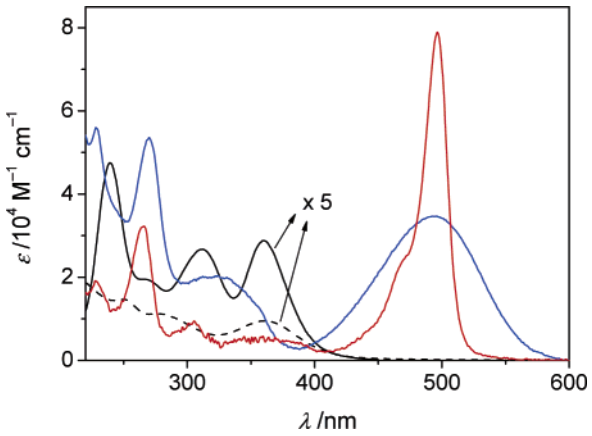

Figure 1. Absorption spectra of $FeCl_3$ (solid black line), $Fe(ClO_4)_3$ (dashed black line), and the title compounds **2** (blue) and **3** (red) in MeCN. The spectra of the salts were multiplied by a factor of 5.

storage, and balance being tightly regulated in an organism.[15] The lack of suitable fluorescent iron indicators is even more obvious when judged in terms of application-oriented features. The receptors employed are often synthetically demanding analogues of ferrichromes or siderophores and, due to the paramagnetic nature of ionic iron, the indication is mostly signaled by fluorescence quenching. To the best of our knowledge, molecular probes that selectively show Fe^{III}-amplified fluorescence in protic solvents have not been reported yet.

When aiming at the rational development of specific molecular reporters for target transition metal ions, the choice of the binding motif is a critical factor. At the cellular level, chemically closely related metal ions frequently are transported by the same or very similar proteins, and thus, for instance, Zn^{II} or Cu^{II} can interfere with iron binding and transport.[16] Therefore, the strategy that we followed to reach the goal of selective Fe^{III}-amplified fluorescence signaling equally relied on careful considerations of the binding preferences of the biochemically important transition metal ions and on the choice of a powerful fluorophore as well as a robust supramolecular architecture of the probe. On one hand, the latter is essential in the sense that it should prevent undesired communication between guest and host during the lifetime of the excited state to avoid unspecific quenching by electron transfer between paramagnetic ion and fluorophore; yet the probe's architecture should facilitate efficient signaling. On the other hand, aqueous as well as organic solutions of dissolved iron salts are colored and show substantial absorption in the UV/near-visible spectral range so that the chromophore should absorb and emit further to the red (Figure 1).

The selection of the receptor unit was driven by our experience in the design of tailor-made *N*-phenyl-substituted

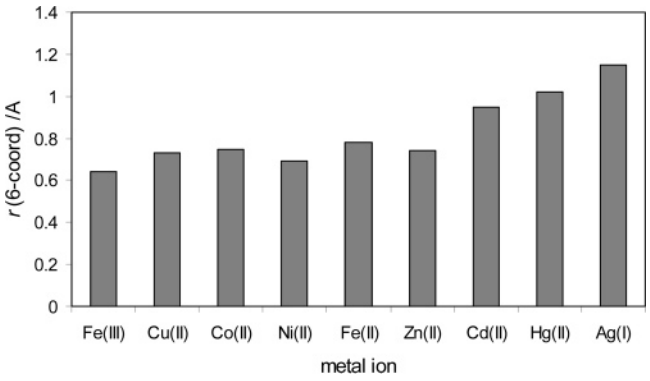

Figure 2. Ionic radii (Å; for six-coordination) of the metal ions employed in our studies.[21] The radius of the simple all-oxygen 12-crown-4 analogue of $AT_2$12C4 was estimated to 0.6−0.7 Å.[22]

Chart 1

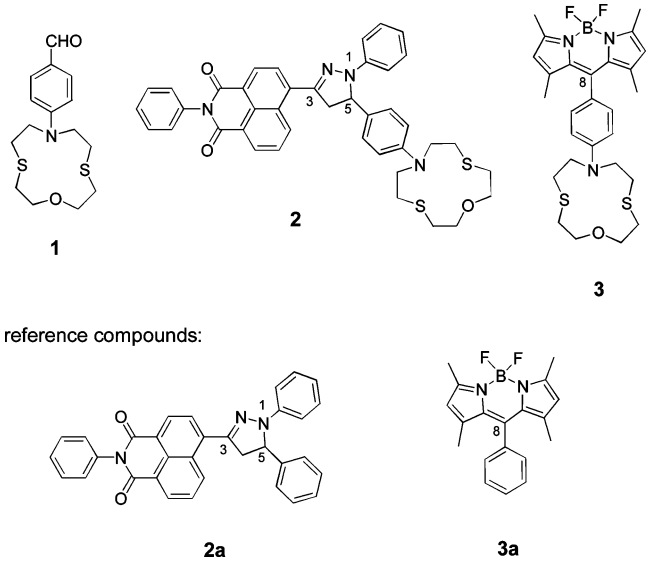

reference compounds:

mixed-donor atom (N,S,O) macrocycles.[17] Further functionalization of such crowned anilines is usually straightforward and thus allows facile integration of these simple receptor modules to a great variety of supramolecular signaling architectures. Targeting Fe^{III}, the wealth of knowledge on synthetic non-heme iron enzyme mimics[18] suggested that a size-restricted aza-oxa-thia macrocycle might be a promising candidate to achieve the required discrimination against other small but more aminophilic or larger and "softer" transition metal ions (for size relations, see Figure 2). Accordingly, we synthesized the crowned benzaldehyde **1**, containing the 1-oxa-4,10-dithia-7-aza-cyclododecane or $AT_2$12C4 macrocycle, and integrated it to two types of fluoroionophores (**2**,**3**) (Chart 1) that have been recently identified by us as suitable platforms to obtain enhanced emission output in the desired wavelength region upon binding to a well-known fluorescence quencher such as Hg^{II}.[19,20]

(12) In the past few years, several researchers have also successfully employed modified fluorescent ligands that either bind to a large number of metal ions (e.g., 8-hydroxyquinoline) or that are usually used for the indication of other cations (e.g., calcein) for the fluorometric monitoring of ionic iron, see: Thomas, F.; Serratrice, G.; Beguin, C.; Aman, E. S.; Pierre, J. L.; Fontecave, M.; Laulhere, J. P. *J. Biol. Chem.* **1999**, *274*, 13375−13383. Pierre, J. L.; Baret, P.; Serratrice, G. *Curr. Med. Chem.* **2003**, *10*, 1077−1084. Ali, A.; Zhang, Q.; Dai, J.; Huang, X. *BioMetals* **2003**, *16*, 285−293.

(13) Aisen, P.; Wessling-Resnick, M.; Leibold, E. A. *Curr. Opin. Chem. Biol.* **1999**, *3*, 200−206. Eisenstein, R. S. *Annu. Rev. Nutr.* **2000**, *20*, 627−662.

(14) Andrews, N. C. *N. Engl. J. Med.* **1999**, *341*, 1986−1195. Touati, D. *Arch. Biochem. Biophys.* **2000**, *373*, 1−6.

(15) Cairo, G.; Pietrangelo, A. *Biochem. J.* **2000**, *352*, 241−250. Beutler, E.; Felitti, V.; Gelbart, T.; Ho, N. *Drug Metab. Dispos.* **2001**, *29*, 495−499.

(16) Askwith, C.; Kaplan, J. *Trends Biochem. Sci.* **1998**, *23*, 135−138.

(17) Rurack, K.; Bricks, J. L.; Reck, G.; Radeglia, R.; Resch-Genger, U. *J. Phys. Chem. A* **2000**, *104*, 3087−3109. Rurack, K.; Koval'chuck, A.; Bricks, J. L.; Slominskii, J. L. *J. Am. Chem. Soc.* **2001**, *123*, 6205−6206. Descalzo, A. B.; Martínez-Máñez, R.; Radeglia, R.; Rurack, K.; Soto, J. *J. Am. Chem. Soc.* **2003**, *125*, 3418−3419. Ros-Lis, J. V.; Martínez-Máñez, R.; Rurack, K.; Sancenón, F.; Soto, J.; Spieles, M. *Inorg. Chem.* **2004**, *43*, 5183−5185.

(18) Mascharak, P. K. *Coord. Chem. Rev.* **2002**, *225*, 201−214. Kovacs, J. A. *Chem. Rev.* **2004**, *104*, 825−848.

(19) Rurack, K.; Resch-Genger, U.; Bricks, J. L.; Spieles, M. *Chem. Commun.* **2000**, 2103−2104.

(20) Rurack, K.; Kollmannsberger, M.; Resch-Genger, U.; Daub, J. *J. Am. Chem. Soc.* **2000**, *122*, 968−969.

Scheme 1. Synthetic Scheme of the Preparation of **1**−**3**[a]

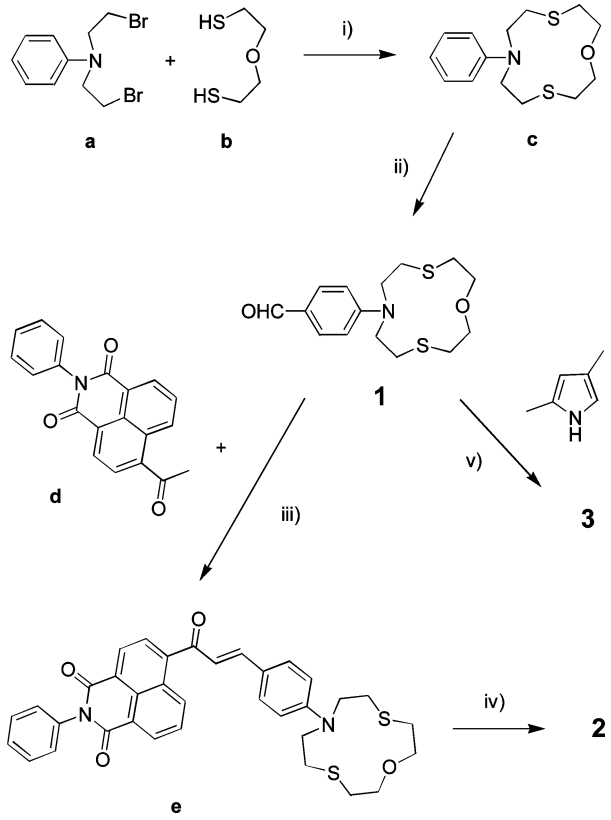

[a] Reagents and conditions: i) NaO*i*Pr/*i*PrOH; ii) $POCl_3$/DMF; iii) piperidine/abs. EtOH; iv) phenylhydrazine hydrochloride/AcOH; v) v.i) CH_2Cl_2/TFA, v.ii) DDQ, v.iii) BF_3·OEt_2, diisopropylethylamine.

Results and Discussion

Synthesis. For the preparation of the phenyl-appended receptor unit **c**, we employed modified reactions based on the chemistry that was utilized to synthesize the parent macrocycle[23] as well as several *N*-alkylated derivatives[24] (Scheme 1). Formylation of **c** then afforded **1**.[25] The crowned benzaldehyde was subsequently transformed into the 1,3,5-triaryl-Δ^2-pyrazoline **2** via the intermediate chalcone **e** as well as into the *meso*-substituted boron-dipyrromethene **3** via a one-pot reaction by successive use of 2,4-dimethylpyrrole, trifluoroacetic acid (TFA), dichloro-dicyano-benzoquinone (DDQ), and BF_3·OEt_2. The syntheses of the model compounds **2a** and **3a** that carry a phenyl group instead of the anilino crown have been published previously by us.[19,26]

Spectroscopic Properties of 2. The 1,3,5-triaryl-Δ^2-pyrazoline[27] **2** was primarily prepared by us to get a profound picture of complex formation with Fe^{III}. The 1,3,5-substitution of the central five-membered Δ^2-pyrazoline ring results in an optimal preorientation of the three subunits in terms of spectroscopic recognition features typically displayed by photoinduced electron transfer (PET) probes.[28] Whereas the N(1)-phenyl donor and the 3-(*N*-phenyl)naphthalimide acceptor are rather planar and electronically conjugated, the phenyl-$AT_2$12C4 receptor at the sp^3-hybridized C(5) is bent in a pseudospiro-like conformation (a twist angle of ∼80° between both molecular planes has been found for similar molecules)[27b] and cannot directly interact electronically with the 1,3-chromophore. Moreover for **2**, in particular, the high conjugation of 1- and 3-substituent in combination with the strong 3-(*N*-phenyl)naphthalimidyl acceptor guarantees to obtain broad and well-separated charge-transfer absorption and emission bands in the red/far-red spectral region at ca. 500 and 680 nm in highly polar solvents such as acetonitrile or alcohols (Figure 3, Table 1).[19] The composite nature of the architecture of **2** is further evident from the absorption spectrum shown in Figure 3. The spectrum is a linear combination of the transition localized on the 1,3-chromophore at ca. 500 nm and the characteristic transition localized on the substituted alkylaminophenyl fragment at ca. 265 nm. Since the 5-anilino receptor is also a strong electron donor, in the unbound state, a fast excited-state PET process from the 5-fragment to the 3-acceptor can compete with the CT in the conjugated 1,3-

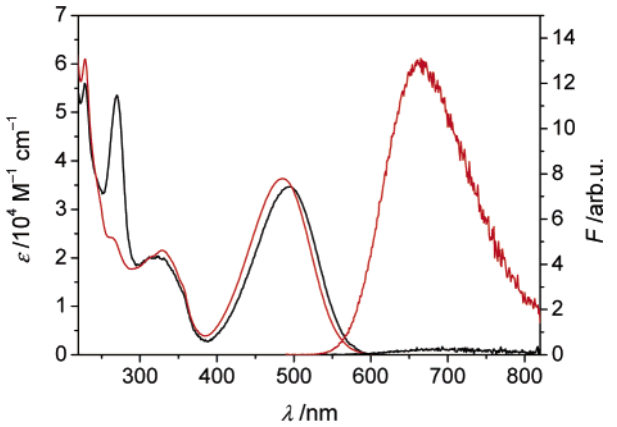

Figure 3. Absorption and emission spectra of **2** (black) and **2a** (red) in MeCN at 298 K.

Table 1. Selected Spectroscopic Data of **2**, Its Complexes, and **2a** in Different Solvents at 298 K[a]

	solvent	λ_{abs} nm	ϵ_{abs} M^{-1} cm^{-1}	λ_{em} nm	Φ_f	τ_f ns
2	MeCN	493	34,600[b]	677	0.004	0.04
2	MeOH	502	30,900[b]	692	0.002	0.02
2−Fe^{III}	MeCN	477	38,100	662	0.12	1.50
2−Fe^{III}	MeOH	491	32,800	688	0.008	0.10
2−Cu^{II}	MeCN	478	37,900	663	0.14	1.72
2a	MeCN	484	36,400[b]	670	0.18	1.32
2a	MeOH	493	34,600[b]	703	0.011	0.16
2a/Fe^{III}	MeCN[c]	714	75,000	–	–	–

[a] $c_{dye} = 3 \times 10^{-6}$ M, $\lambda_{exc} = 480$ nm. Counteranion perchlorate. [b] The reduction in molar absorptivity is due to the fact that the spectra are broader in MeOH as compared to those in MeCN. The oscillator strengths, i.e., the integrals of the longest-wavelength absorption bands, however, are virtually identical for each dye in both solvents. [c] Fe^{III} does not trigger Knorr's reaction in (neutral) methanol which is conceivable with its reduced oxidizing power in this solvent and based on the fact that Knorr's test works only in the presence of acids in protic solvents.[29]

(21) Shannon, R. D. *Acta Crystallogr.* **1976**, *32A*, 751−767.
(22) Dalley, N. K. In *Synthetic Multidentate Macrocyclic Compounds*; Izatt, R. M., Christensen, J. J., Eds.; Academic Press: New York, 1978; pp 207−243.
(23) Black, D. S. C.; McLean, I. A. *Tetrahedron Lett.* **1969**, *45*, 3961−3964.
(24) Shinkai, S.; Shigematsu, K.; Honda, Y.; Manabe, O. *Bull. Chem. Soc. Jpn.* **1984**, *57*, 2879−2884. Youinou, M.-T.; Osborn, J. A.; Collin, J.-P.; Lagrange, P. *Inorg. Chem.* **1986**, *25*, 453−461.
(25) Adapted from Ross, W. C. J. *J. Chem. Soc.* **1949**, 183−191.
(26) Kollmannsberger, M.; Rurack, K.; Resch-Genger, U.; Daub, J. *J. Phys. Chem. A* **1998**, *102*, 10211−10220.
(27) (a) de Silva, A. P.; Gunaratne, H. Q. N.; Lynch, P. L. M. *J. Chem. Soc., Perkin Trans. 2* **1995**, 685−690. (b) Rurack, K.; Bricks, J. L.; Schulz, B.; Maus, M.; Reck, G.; Resch-Genger, U. *J. Phys. Chem. A* **2000**, *104*, 6171−6188. (c) Fahrni, C. J.; Yang, L.; VanDerveer, D. G. *J. Am. Chem. Soc.* **2003**, *125*, 3799−3812.
(28) (a) Bissell, R. A.; de Silva, A. P.; Gunaratne, H. Q. N.; Lynch, P. L. M.; Maguire, G. E. M.; Sandanayake, K. R. A. S. *Chem. Soc. Rev.* **1992**, *21*, 187−195. (b) Rurack, K.; Resch-Genger, U. *Chem. Soc. Rev.* **2002**, *31*, 116−127.

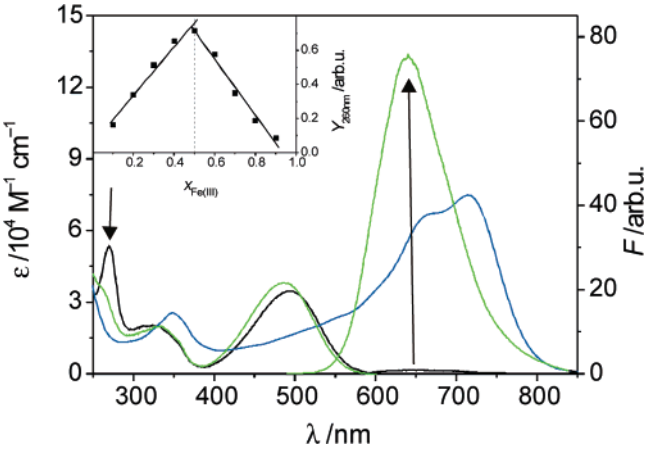

Figure 4. Absorption and emission spectra of **2** (black), **2**−Fe^{III} (green), and the reaction product of **2a** and Fe^{III} in MeCN (blue); arrows indicate the changes measured for **2** upon addition of Fe^{III}. (Inset) Plot according to the Method of Continuous Variations,[30] indicating the 1:1 stoichiometry of **2**−Fe^{III}.

chromophore. As a consequence, the fluorescence of **2** is drastically quenched as compared to that of model dye **2a** that lacks an electron-rich 5-substitutent, with the band position remaining virtually unchanged (Figure 3, Table 1). For instance, based on the data given in Table 1 and a formalism described in ref 27b, the rate constant of the nonadiabatic intramolecular electron-transfer process is determined to $k_{ET} = 3.05 \times 10^{10}$ ns^{-1} in acetonitrile. In protic solvents such as methanol, not only is the fluorescence of **2** strongly quenched, but the emission of **2a** is also considerably reduced (Table 1). These findings are obviously related to previous observations by us that Δ^2-pyrazolines with such strong 3-acceptors tend to suffer from fluorescence quenching due to hydrogen-bonding interactions with solvent molecules in alcohols.[27b]

Complexation Features of 2. Employing **2** and **2a** allowed us to follow the complexation characteristics of the phenyl-AT$_2$12C4 moiety in more detail. First, binding of the target ion at the crown engages the lone electron pair of the receptor's anilino nitrogen atom in coordination and thus leads to a decrease of the characteristic absorption band at 265 nm for **2** (Figure 4). Second, the electron-donating potential of the 5-receptor is drastically reduced in its bound state, leading to a suppression of the PET process and amplified fluorescence with only minor spectral shifts (Figure 4). The inset of Figure 4 indicates a 1:1 stoichiometry, and formation of the strong complex (log $K > 5.5$) is immediate. As a cross-check, the UV/vis spectra of reference compound **2a**, carrying an unsubstituted phenyl group at the 5-position, were followed upon addition of Fe^{III} in acetonitrile. Already at equimolar ratios, the color of the solution is deep blue (Figure 4), conceivable with a redox reaction which is known as Knorr's Pyrazoline Test.[29] The product of this test is a planar bis(1-[3-aryl-Δ^2-pyrazolinyl])-biphenyl dication with extended electron delocalization in the entire chromophore,[29c] exemplified by the intense near-IR absorption. ESR measurements provided further insight into the coordination mode (Figure 5). Whereas Fe(ClO$_4$)$_3$ dissolved in acetonitrile is largely ESR-silent under the experimental conditions used here, gradual formation of **2**−Fe^{III} leads to the

(29) (a) Knorr, L.; Laubmann, H. *Chem. Ber.* **1888**, *21*, 1205−1212. (b) Knorr, L. *Chem. Ber.* **1893**, *26*, 100−103. (c) Pragst, F.; Vieth, B. *Z. Phys. Chem.* **1976**, *275*, 849−867.

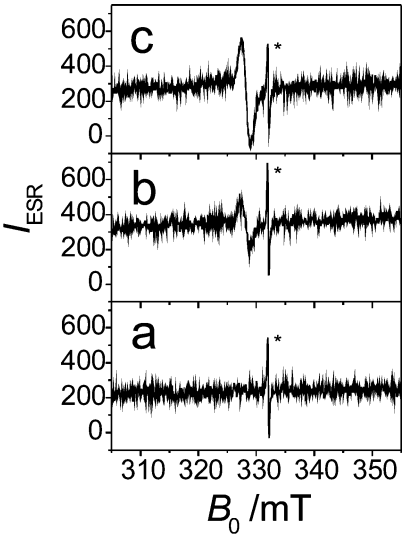

Figure 5. ESR spectra of (a) Fe^{III} in MeCN and Fe^{III}:**2** = 2 (b) and = 1 (c). The asterisk indicates the resonance of a MgO/Cr^{3+} standard at $g' = 1.9796$.

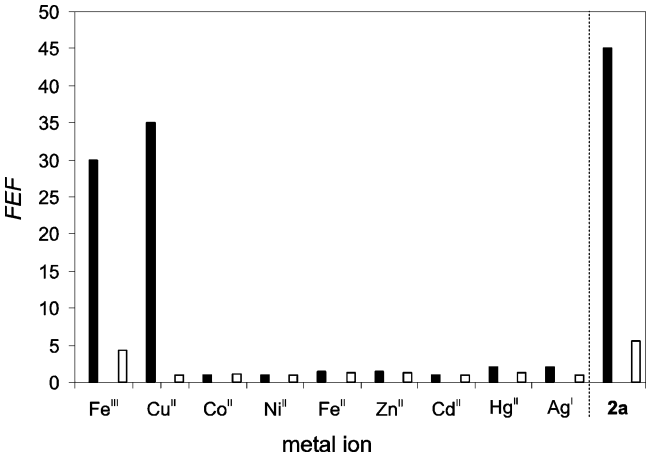

Figure 6. Fluorescence enhancement factors for **2** in the presence of various transition metal ions in MeCN (black; equimolar amounts of metal ions) and MeOH (white; 5-fold excess of metal ions). The relative fluorescence yield of **2a** vs **2** in both solvents is included on the far right for comparison, see Table 1 for actual fluorescence quantum yield data.

appearance of a narrow resonance at $g' = 2.0037$ ($\Delta B_{pp} = 1$ mT), suggesting low-spin complexation in analogy to tetra (or penta-)-dentate Fe^{III} complexes with mixed donor−atom ligation and one (or two) weakly bound sixth ligand(s), e.g., ClO_4^-.[18]

2 displays favorable selectivity features already in acetonitrile. Whereas an equimolar amount of Fe^{III} induces a ca. 30-fold increase in fluorescence, Ni^{II}, Co^{II}, and Cd^{II} are entirely silent, Zn^{II} and Fe^{II} lead to a 1.5-fold and Hg^{II} and Ag^{I} to a 2-fold enhancement. Only Cu^{II} yields equally amplified emission in MeCN (Figure 6). Upon taking a step toward protic solvents, the spectroscopic characteristics of the host−guest reaction between **2** and Fe^{III} remain virtually identical. Binding of the cation leads to increased emission due to the formation of a 1:1 complex with log $K = 4.9$. The reduced fluorescence enhancement factor found in methanol as compared to the aprotic solvent is in accordance with the considerably low fluorescence quantum yield of **2a** in methanol and the mechanistic implications described above (Figure 6, Table 1). Furthermore, in methanol, no enhanced fluorescence could be

Table 2. Spectroscopic Data of **3** and **3a** in Different Solvents at 298 K[a]

	solvent[b]	λ_{abs} nm	fwhm[c] nm	ϵ_{max} M^{-1} cm^{-1}	λ_{em} (LE/CT)[d] nm	fwhm[c] nm	Φ_f[e]	Φ_f^{CT}/Φ_f^{LE}	τ_f ns
3	MeCN	497	23	79,200	508/−	25	0.0003	−	<0.003
	MeOH	497	22	78,700	510/−	26	0.0008	−	<0.003
	H_2O	505	59	34,800	508/635	43/123	0.022	21	0.30/1.94[f]
	MOPS	506	59	36,700	508/634	52/121	0.026	11.3	0.18/3.03[f]
	Tris/HCl	508	61	33,100	509/632	49/124	0.027	10.0	0.17/3.09[f]
3a[g]	MeCN	497	21	83,100	505/−	25	0.60	−	3.17
	MeOH	498	19	80,600	508/−	23	0.65	−	3.21

[a] $c_{dye} = 1 \times 10^{-6}$ M, $\lambda_{exc} = 470$ nm for steady-state and 480 nm for time-resolved fluorescence measurements. [b] MOPS (3-[*N*-morpholino]propane sulfonic acid) buffer, adjusted to pH 5.1; Tris (tris-(hydroxymethyl) amino methane)/HCl buffer, adjusted to 5.8. [c] Full width at half-maximum. [d] First maximum corresponds to the typical BDP-localized band, second one to the charge-transfer band. [e] Overall fluorescence quantum yield. [f] Major decay components in the blue (= LE) and red (= CT) part of the emission spectrum; for a detailed description of such dual emission features, see refs 26,33. [g] **3a** is only very weakly soluble in water and shows strong tendencies of aggregation already at lower micromolar concentrations.

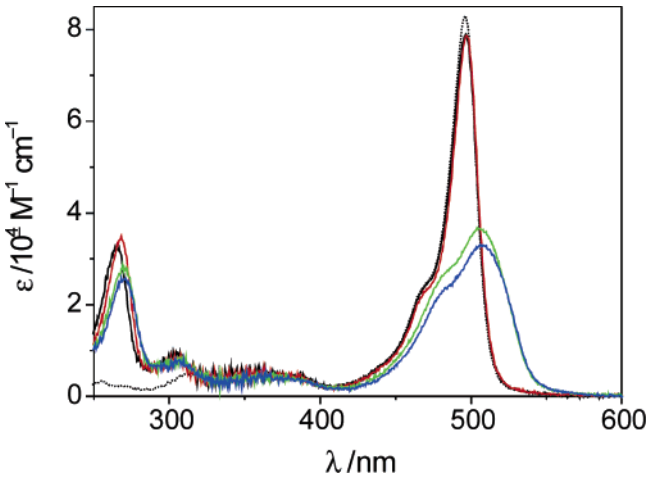

Figure 7. Absorption spectra of **3** in MeCN (black), MeOH (red), 0.01 M MOPS-buffered (green), and 0.01 M Tris/HCl-buffered (blue) aqueous solution. The absorption spectrum of **3a** in MeCN (dotted line) is included for comparison.

detected for Cu^{II}, and all the other metal ions also do not show any competition (Figure 6).

These results distinguish the $AT_2$12C4 macrocycle as a suitable receptor for Fe^{III} and suggest that sensor molecules with electronically decoupled, rigidly fixed, and sterically preoriented architectures are largely immune against the inherently quenching nature of paramagnetic metal ions. However, as the solubility of **2** is very limited in aqueous media and as these Δ^2-pyrazolines principally suffer from fluorescence quenching in alcohols, another type of decoupled, rigid, and preoriented probe scaffold was chosen to obtain an Fe^{III}-selective indicator that operates in aqueous solutions, the *meso*-substituted boron-dipyrromethene (BDP) platform.[20,26,28b,31]

Spectroscopic and Complexation Properties of 3 in Non-aqueous Solvents. Figure 7 reveals that in **3**, due to methyl group substitution at the 1,7-positions of the BDP core, the crowned aniline in the 8- or *meso*-position is also electronically decoupled from the main fluorophore, resulting in a linear combination of the absorption bands as described above for **2**. The spectral absorption features of **3** are thus very similar to those of **3a** and typical for such BDP dyes, e.g., $\lambda_{abs} = 497$ nm, $\epsilon \approx 79{,}000$ M^{-1} cm^{-1} in organic solvents (Table 2). Moreover, in the unbound state, the typical BDP fluorescence of **3** at e.g. 508 nm in MeCN is strongly quenched due to an ultrafast charge-transfer (CT) process from the electron-rich 8-anilino receptor moiety to the electron-accepting BDP (Table 2). In highly polar solvents, the CT process occurs almost quantitatively, and due to the forbidden nature of CT emission from perpendicularly oriented ensembles,[32] only a weak BDP-localized (or locally excited, LE) emission and no CT fluorescence can be found.[20,26] For instance, the fluorescence quantum yield of **3** in solvents such as MeCN and MeOH is ca. 10^{-4}, orders of magnitude lower than that of the 8-phenyl analogue **3a** ($\Phi_f \approx 0.6$).[26] Although strongly quenched, the spectral shape in fluorescence of **3** is again virtually identical to that of **3a**, reflecting the decoupled architecture of the sensor molecule.

Addition of Fe^{III} to **3** in MeCN accordingly leads to a drastic increase in LE fluorescence with typical PET features such as a virtually unchanged band position (Figure 8) and mono-exponential decay kinetics close to that of the model dye, $\tau_f = 2.95$ vs 3.17 ns for **3**−Fe^{III} vs **3a** (Table 3). In this solvent, the ion selectivity is similar to that of **2** (Figure 9), with Cu^{II} leading also to strongly enhanced fluorescence (τ_f[**3**−Cu^{II}] = 2.79 ns). Emerging to MeOH, the spectral and switching features of **3** in the presence of Fe^{III} are preserved (τ_f[**3**−Fe^{III}] = 2.71 ns; Figure 8). However, Cu^{II} is now less strongly bound, yielding only a slight fluorescence enhancement and a biexponential decay with two shorter lifetimes (Figure 9, Table 3), indicative of the formation of two weak complexes of different conformation related to the endo/exo isomerization of *N*-substituted aza crowns.[34] Such a behavior has been found by us before for some of the complexes of alkali- and alkaline-earth metal ions and a BDP dye carrying a *N*-phenyl-monoaza-tetraoxa-15-crown-5 unit at the 8-position.[26] The behavior is based on the fact that the excited state CT process in 8-anilino-substituted BDPs is exceptionally sensitive to changes in the electron-donating ability of the unit in the *meso*-position, also exemplified by the remarkably high FEF that can be obtained upon cation binding in dyes such as **3**.[20,26] As in the case of **2**, all the other potential competitors remain silent in MeOH (Figure 9). The complex formation features of **3** and Fe^{III} in both organic solvents reflect the results found for **2** and the target metal ion, i.e. complexation is immediate with log $K > 5.5$ in MeCN and 4.8 in MeOH and 1:1 stoichiometries (Figure 8).

(30) Vosburgh, W. C.; Cooper, G. R. *J. Am. Chem. Soc.* **1941**, *63*, 437−442.
(31) Kollmannsberger, M.; Gareis, T.; Heinl, S.; Breu, J.; Daub, J. *Angew. Chem., Int. Ed. Engl.* **1997**, *36*, 1333−1335. Gareis, T.; Huber, C.; Wolfbeis, O. S.; Daub, J. *Chem. Commun.* **1997**, 1717−1718.
(32) Rettig, W. *Top. Curr. Chem.* **1994**, *169*, 253−299.
(33) Schuddeboom, W.; Jonker, S. A.; Warman, J. M.; Leinhos, U.; Kühnle, W.; Zachariasse, K. A. *J. Phys. Chem.* **1992**, *96*, 10809−10819. Leinhos, U.; Kühnle, W.; Zachariasse, K. A. *J. Phys. Chem.* **1991**, *95*, 5, 2013−2021.
(34) Gokel, G. W.; Echegoyen, L.; Kim, M. S.; Eyring, E. M.; Petrucci, S. *Biophys. Chem.* **1987**, *26*, 225−233. Echegoyen, L.; Gokel, G. W.; Kim, M. S.; Eyring, E. M.; Petrucci, S. *J. Phys. Chem.* **1987**, *91*, 3854−3862.

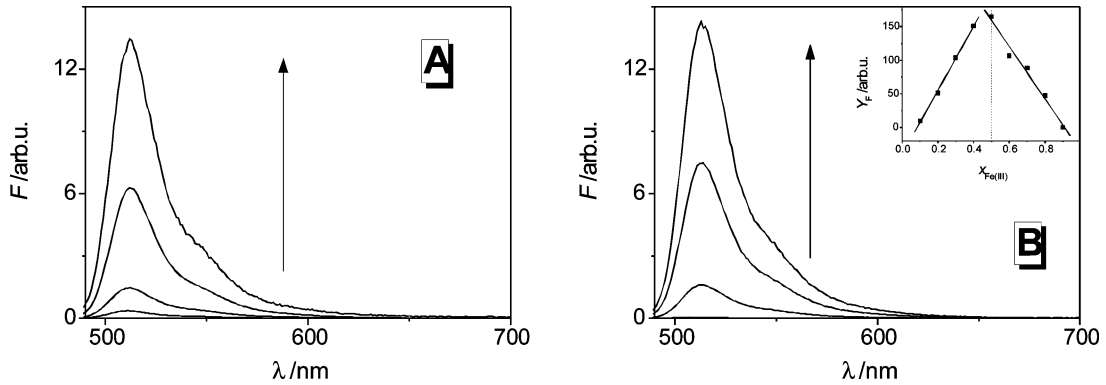

Figure 8. Fluorescence titration spectra of **3** with Fe^{III} in MeCN (A) and MeOH (B). (Inset) Plot according to the Method of Continuous Variations,[30] indicating the 1:1 stoichiometry of **3**−Fe^{III}.

Table 3. Spectroscopic Data of the Complexes of **3** in Different Solvents at 298 K[a]

	solvent[b]	λ_{abs} nm	fwhm[c] nm	ϵ_{max} M^{-1} cm^{-1}	λ_{em} nm	fwhm[c] nm	FEF$^{LE\,d}$	τ_f ns
3−Fe^{III}	MeCN	498	22	80,300	512	27	>500	2.95
3−Fe^{III}	MeOH	498	22	80,200	513	27	>500	2.71
3−Fe^{III}	H_2O	506	62	31,800	510	31	14	3.48
3−Fe^{III}	MOPS	508	63	33,400	512	31	14	3.40
3−Fe^{III}	Tris/HCl	510	65	30,600	511	30	15	3.54
3−Cu^{II}	MeCN	500	22	80,500	512	27	>500	2.79
3−Cu^{II}	MeOH	497	22	78,700	510	26	~10	0.24, 1.25[e]

[a−c] See Table 2. [d] Cation-induced fluorescence enhancement factor for the BDP (LE) emission, for respective data of unbound **3**, see Table 2. [e] Biexponential decay of the LE band, most probably due to the formation of two complexes with different conformation as has been observed before for various main group metal ions and another *meso*-substituted BDP probe in ref 26. The relative amplitudes are $a_{rel}[0.24] = 0.83$ and $a_{rel}[1.25] = 0.17$.

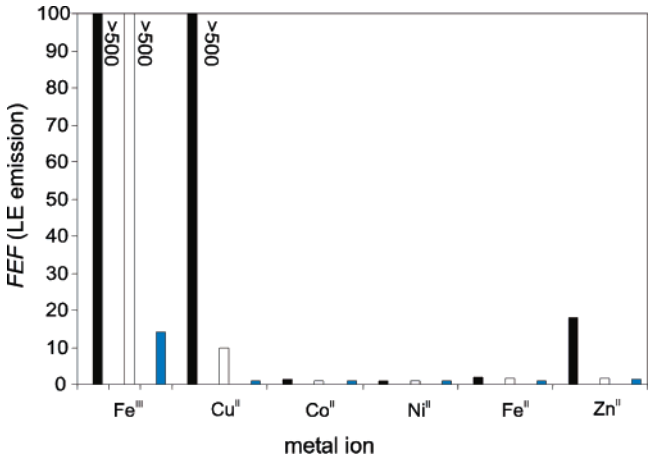

Figure 9. Enhancement factors for the LE fluorescence of **3** in the presence of the biochemically important transition metal ions of the first row in MeCN (black), MeOH (white), and water (blue). The response toward the metal ions in the buffered solutions is similar to that in water; see also Table 3 for **3**−Fe^{III}.

Spectroscopic and Complexation Properties of 3 in Aqueous Solution. In neat as well as buffered (0.01 M MOPS or Tris/HCl) aqueous solution, the absorption features of **3** are slightly changed. The intensity of the molecular C−C frame vibration of 1300 cm^{-1}, which is typical for BDPs, is enhanced, and the spectra are thus slightly broadened (Figure 7). However, although the molar absorptivity at the maximum is reduced in aqueous solution, the integral absorption of the typical lowest-energy transition localized on the BDP fragment is virtually unchanged (Table 2). Most importantly, **3** shows dual emission in all of these aqueous solutions (Figure 10). The maxima of

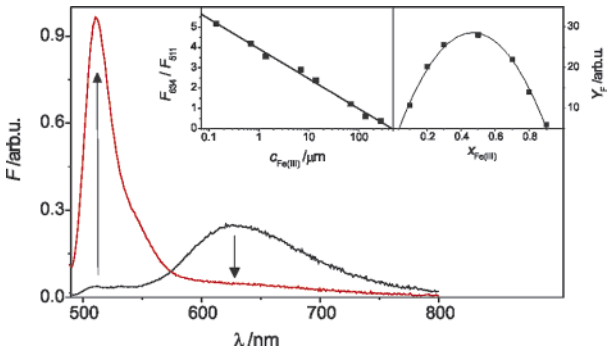

Figure 10. Fluorescence spectra of **3** (black) and **3**−Fe^{III} (red) in 0.01 M MOPS buffer. The arrows indicate the changes upon complexation. The ratiometric signal F_{634}/F_{511} of a typical titration is included as the left inset ($r^2 = 0.994$), a plot according to the Method of Continuous Variations[30] in water as the right inset. Note that Continuous Variations plots tend to flatten as the complex stability decreases; see, for example a recent discussion in ref 43.

the BDP-localized LE band and the charge transfer (CT) band are found at 508 ± 1 and 634 ± 2 nm, respectively, with overall $\Phi_f = 0.025 \pm 0.003$. The ratio of Φ_f[CT]/Φ_f[LE] is 21 in neat water and 11 ± 1 in the buffers. Apparently, water is also strongly solvating the receptor unit so that high quenching rates as in MeCN or MeOH ($\Phi_f \approx 10^{-4}$) cannot be achieved. Nonetheless, the interaction of the solvent with the anilino nitrogen is weak enough to generate the red-shifted CT emission, suggesting that **3** might be suitable for analytically advantageous ratiometric sensing.[35] Indeed, titration with Fe^{III} results in a displacement of water molecules from the receptor, entailing an increase of the typical BDP emission and a concomitant decrease of the CT band (Figure 10). Besides these favorable ratiometric signaling features, **3** indicates Fe^{III} by a strong enhancement of BDP fluorescence. Concerning selectivity and interference in aqueous solution, **3** displays negligible response to the cations listed before, including Cu^{II} (Figure 9). Complexation of Fe^{III} by **3** is again immediate in neat water as well as the buffered solutions, and the complexes of 1:1 stoichiometry possess log $K = 4.2$, 4.0, and 4.1 in H_2O, 0.01 M MOPS, and 0.01 M Tris/HCl buffer, respectively.

Conclusion

In this contribution, we have introduced a receptor unit that allows selective detection of Fe^{III} in various media. By integra-

(35) Silver, R. B. *Methods Cell Biol.* **1998**, *56*, 237−251. Dustin, L. B. *Clin. Appl. Immunol. Rev.* **2000**, *1*, 5−15.

tion of the unit to two decoupled and rigid molecular architectures, we obtained, to our knowledge, the first examples of fluorescent probes that selectively show Fe^{III}-amplified emission. One of the sensor molecules even allows for ratiometric signaling in aqueous solution with both bands well within the visible range of the spectrum. Although the complex stability constants of the couple AT_212C4/Fe^{III} are only moderate in neat and buffered aqueous solutions, the exceptional sensitivity of the signaling reaction in the boron-dipyrromethene-type probe **3** still allows detection of the target cation in the lower micromolar range. On one hand, such a strategy might be valuable in designing probes that only indicate the "free" or labile ionic form of transition metals in a sample or environment,[36] without liberating the cation from naturally occurring biotic or abiotic complexes, removing it from a system or saturating the molecular sensor by irreversible complex formation. On the other hand, emerging from the present structure to lariat-type macrocyclic receptors that are equipped with one or two pendant arms to satisfy the need of the ion for six-coordination should lead better to related systems with increased complex stabilities. However, concerning the latter step of modification, it should be kept in mind that increasing denticity of the chelating moieties of iron-sensitive probes might result in drawbacks in selectivity.[37] In summary, we believe that the studies presented here will stimulate further research in the area of fluorescent sensor molecules for other largely neglected metal ions such as Co^{II}, Fe^{II}, or Mn^{II}.

Experimental Section

Materials. All the solvents employed were of UV-spectroscopic grade and purchased from Aldrich. Metal perchlorates and $FeCl_3$ purchased from Merck, Acros, and Aldrich were of highest purity available and dried as described previously. **Caution:** Perchlorate salts present a potenital explosion hazard and should be handled with care and possibly only in small quantities. The spectroscopic response of **2** and **3** in the presence of Fe^{III} was independent of the counteranion used, i.e., perchlorate or chloride.

Synthesis. General Methods. The chemical structures of the synthesized compounds were confirmed by elemental analysis, ^{1}H NMR, ^{13}C NMR, and MS, and their purity was checked by reversed phase HPLC (HPLC set up from Merck-Hitachi; RP18 column; acetonitrile/water = 75/25 as eluent) employing UV detection (UV detector from Knaur; fixed wavelength at 310 nm). NMR spectra were obtained with a 500 MHz NMR spectrometer Varian $Unity_{plus}$ 500. The mass spectra were recorded on a Finnigan MAT 95 spectrometer with an ESI-II/APCI-Source for electrospray ionization and the base peaks $[M + Na]^+$ were determined.

4-(1-Oxa-4,10-dithia-7-aza-cyclododec-7-yl)-benzaldehyde (1). As shown in Scheme 1, condensation of **a** and bis-(2-mercaptoethyl)ether in the presence of NaO*i*Pr/*i*PrOH yielded **c**,[23,24] that was then formylated[25] to give **1** in 41% yield.

1-Phenyl-3-(*N*-phenyl-1,8-naphthalimid-4-yl)-5-[4-(1-oxa-4,10-dithia-7-aza-cyclododec-7-yl)-phenyl]-Δ^2-pyrazoline (2). For **e**, a mixture of 4-acetylnaphthalic acid phenylamide[38] **d** (1 mmol), **1** and piperidine was refluxed in absolute ethanol for 8−10 h. After cooling, a solid precipitate was separated, washed with ethanol, purified by column chromatography (silica, dichloromethane, chloroform), and recrystallized. Then, a solution of 0.3 mmol **e** and 0.6 mmol phenylhydrazine hydrochloride in 5 mL of acetic acid was heated for 10 h at 100 °C. The resulting red reaction mixture was poured into 50 mL of ice water and neutralized with 10% aqueous sodium carbonate. The solid precipitate was separated, washed with water, and purified by column chromatography (silica/$CHCl_3$). After evaporation of the solvent, **2** was crystallized from toluene. Dark-red crystals, mp 253−256 °C, yield 35%. ^{1}H NMR ($CDCl_3$) δ (ppm): 2.782−2.811 (**CH$_2$**N, t, J = 4 Hz, 4H); 2.845−2.887 (S−**CH$_2$**−CH$_2$−O, t, J = 6.5 Hz, 4H); 3.355−3.433 (**CH$_2$**C═N, dd, 1H); 3.724−3.754 (S−**CH$_2$**−CH$_2$−N, OCH_2, m, 8H); 4.020−4.118 (**CH$_2$**C═N, dd, 1H); 5.335−5.397 (Ar**CH**N, dd, 1H); 6.875−10.061 (arom. H, 19H). ^{13}C NMR ($CDCl_3$) δ (ppm): 30.520, 32.288 (CH_2−S); 45.126 (CH_2 pyrazoline); 63.109 (ArCHN); 73.455 (CH_2−O); 113.954; 120.250; 121.594; 122,820; 126.210; 127. 098; 127.773; 128.324; 128.684; 128.895; 129.017; 129.164; 129.340; 129.617; 131.029; 131.543; 134.885; 135.432; 135.650; 143.677; 145.310 (arom. C); 164.020, 164.328 (C═O amide). Anal. Calcd for $C_{41}H_{38}N_4O_3S_2$: C 70.46, H 5.48, N 8.02; found C 70.33, H 5.44, N 8.12.

1,3,5,7-Tetramethyl-8-[4-(1-oxa-4,10-dithia-7-aza-cyclododec-7-yl)-phenyl]-4*H*-3a,4a-diaza-4-difluorobora-*s*-indacene (3). The reaction was carried out under nitrogen atmosphere. 0.100 g (0.32 mmol) of **1** were reacted at room temperature with 0.1 mL (0.096 g, 1.0 mmol) of 2,4-dimethylpyrrole in 200 mL of CH_2Cl_2 in the presence of three drops of trifluoroacetic acid (TFA). After complete conversion of the benzaldehyde (TLC-control), 0.073 g (0.32 mmol) of dichloro-dicyano-benzoquinone (DDQ) were added. After stirring for 15 min, 3 mL of both diisopropyl-ethylamine and BF_3·OEt_2 were added. After quenching the reaction with water and extracting with dichloromethane, the organic layer was dried over sodium sulfate, and the solvent was removed in vacuo. Column chromatography on silica using CH_2Cl_2 as solvent yielded 0.028 g (0.053 mmol) of **3**. Orange plates, mp 218−219 °C, yield 17%. ^{1}H NMR ($CDCl_3$) δ (ppm): 1.50 (γ CH_3, s, 6H), 2.54 (α CH_3, s, 6H,), 2.82−2.85 (CH_2, m, 4H), 2.91−2.96 (CH_2, m, 4H), 3.76−3.82 (CH_2, m, 8H), 5.97 (pyrrole-H, s, 2H), 6.70−7.04 (arom. H, m, 4H). ^{13}C NMR ($CDCl_3$) δ (ppm): 14.6 (+), 14.9 (+), 30.6 (−), 32.4 (−), 50.2 (−), 73.7 (−), 111.4 (+), 120.9 (+), 121.9 (q), 129.1 (+), 132.2 (q), 143.1 (q), 143.2 (q), 148.2 (q), 154.7 (q). MS (EI, 70 eV): m/z (%) = 529 (100) [M^+]. Anal. Calcd for $C_{25}H_{34}BF_2N_3O_1S_2$: C 61.24, H 6.47, N 7.93; found C 61.13, H 6.40, N 7.89. FT-IR (KBr) $\tilde{\nu}$ = 2963, 2930, 2868, 1541, 1476, 1316, 1187, 1155, 1074, 978, 825 cm^{-1}.

Optical Spectroscopic Procedures. UV/vis spectra were recorded on a Bruins Instruments Omega 10 spectrophotometer, and for the steady-state fluorescence spectra, a Spectronics Instruments 8100 spectrofluorometer was employed. Titrations were performed on a Perkin-Elmer LS50B spectrofluorometer. All measurements were carried out at 298 ± 1 K and with upper micro- or millimolar stock solutions in MeCN. Molar extinction coefficients were determined from N = 8 individual samples. For the fluorescence experiments, only dilute solutions with an optical density (OD) below 0.1 at the absorption maximum were used, and the fluorescence measurements were performed with a 90° standard geometry and polarizers set at 54.7° (emission) and 0° (excitation). The fluorescence quantum yields (Φ_f) were determined relative to fluorescein 27 in 0.1 N NaOH (Φ_f = 0.90 ± 0.03)[39] and DCM in methanol (Φ_f = 0.43 ± 0.08).[40] All the fluorescence spectra were corrected for the spectral response of the detection system (calibrated quartz halogen lamp placed inside an integrating sphere; Gigahertz-Optik) and for the spectral irradiance of the excitation channel (calibrated silicon diode mounted at a sphere port; Gigahertz-Optik). The uncertainties of the fluorescence quantum yields were determined to ±5% (for $\Phi_f > 0.2$), ±10% (for $0.2 > \Phi_f > 0.02$), ±20% (for $0.02 > \Phi_f > 5 \times 10^{-3}$), and ±30% (for $5 \times 10^{-3} > \Phi_f$), respectively.

(36) Pietrangelo, A. *J. Hepatol.* **2000**, *32*, 862−864.
(37) Esposito, B. P.; Breuer, W.; Cabantchik, Z. I. *Biochem. Soc. Trans.* **2002**, *30*, 729−732.
(38) Adapted from Krasovitskii, B. M.; Afanasiadi, L. M. *Preparativnaya Khimiya Organicheskikh Luminoforov*; Folio: Kharkov, 1997; p 186. The last step in the synthesis of **d** had to be carried out with propionic acid to allow for higher reaction temperatures.
(39) Olmsted, J., III. *J. Phys. Chem.* **1979**, *83*, 2581−2584.
(40) Drake, J. M.; Lesiecki, M. L.; Camaioni, D. M. *Chem. Phys. Lett.* **1985**, *113*, 530−534.

Fluorescence lifetimes (τ_f) were measured with a unique laser impulse fluorometer with picosecond time resolution described by us in an earlier publication[41] and modified according to a description in ref 42. Either the second harmonic output of the Ti:sapphire laser or the frequency quadrupled idler of the OPA were used for excitation. The fluorescence was collected at right angles (polarizer set at 54.7°; monochromator with spectral bandwidths of 4, 8, and 16 nm), and the fluorescence decays were recorded by the single-photon timing method. While realizing typical instrumental response functions of 25−30 ps (full width at half-maximum), the time division was 5.2 ps channel^{-1} and the experimental accuracy amounted to ±3 ps, respectively. The laser beam was attenuated using a double prism attenuator from LTB, and typical excitation energies were in the nanowatt to microwatt range (average laser power). The fluorescence lifetime profiles were analyzed with a PC using the software package Global Unlimited v2.2 (Laboratory for Fluorescence Dynamics, University of Illinois). The goodness of the fit of the single decays as judged by reduced chi-squared (χ_R^2) and the autocorrelation function *C(j)* of the residuals was always below $\chi_R^2 < 1.2$. For **3** in aqueous media, decays were recorded at 10 different wavelengths over the entire emission spectrum and analyzed by global analysis. Such a global analysis of decays recorded at different emission wavelengths implies that the decay times of the species are linked while the program varies the preexponential factors and lifetimes until the changes in the error surface (χ^2 surface) are minimal, i.e., convergence is reached. The fitting results are judged for every single decay (local χ_R^2) and for all the decays (global χ_R^2), respectively. The errors for all the global analytical results were below a global $\chi_R^2 = 1.2$.

Method of Continuous Variations.[30] For a continuous variations diagram, the difference Y_λ between the measured absorbance A_λ and the calculated absorbance A_λ' is plotted vs the molar fraction x of one reactand. The absorbances measured for the pure solutions of metal salt (subscript M) and probe (subscript P) are used to calculate A_λ' according to eq 1. In the experiment, solutions of different molar ratios are prepared from equimolar solutions of M and P and the actual absorbance A_λ is measured. Then, Y_λ is calculated (eq 2), and when plotting Y_λ vs x_M, a maximum at 0.5 corresponds to a complex of 1:1 stoichiometry, respectively (see inset of Figure 4).

$$A'_\lambda = x_M \epsilon(\lambda)_M c_M d + x_P \epsilon(\lambda)_P c_P d \quad (1)$$

$$Y_\lambda = A_\lambda - A'_\lambda \quad (2)$$

with $c_{M0} = c_{P0}$ and $x_M + x_P = 1$; d is the optical path length. Alternatively, continuous variations diagrams can be constructed from fluorescence data in a similar fashion (see inset of Figure 8).

ESR Spectroscopy. ESR spectra were recorded with an ERS300 spectrometer (Zentrum für Wissenschaftlichen Gerätebau, Berlin) at X-band frequencies with 20 mW microwave power at 300 K, respectively. Measurements were performed in narrow silica capillaries ("Q-band tubes"). For the complexation experiments, **2** and $Fe(ClO_4)_3$ of highest purity available were dissolved in acetonitrile at 1.2×10^{-4} M (concentration is limited by the solubility of the probe), and the respective metal-to-probe ratios were accordingly adjusted by mixing of the metal solution with either **2** in MeCN or pure MeCN.

Acknowledgment. Financial support by the Deutsche Forschungsgemeinschaft DFG, the Studienstiftung des Deutschen Volkes, and BAM's Ph.D. Program is gratefully acknowledged. The work is part of the Graduate College "Sensory Photoreceptors in Natural and Artificial Systems" (DFG, GRK 640, University of Regensburg). We thank M. Spieles (BAM) for experimental help.

JA050652T

(41) Resch, U.; Rurack, K. *Proc. SPIE-Int. Soc. Opt. Eng.* **1997**, *3105*, 96−103.
(42) Shen, Z.; Röhr, H.; Rurack, K.; Uno, H.; Spieles, M.; Schulz, B.; Reck, G.; Ono, N. *Chem. Eur. J.* **2004**, *10*, 4853−4871.
(43) Sayao, A.; Boccio, M.; Asuero, A. G. *Int. J. Pharm.* **2005**, *295*, 29−34.